Analogy Of The Losses In Surface And Interior Permanent Magnet Synchronous Wind Turbine Generators

Mr. Dhas Bensam Samraj, Dr. Maruthu Pandi Perumal

Abstract: This paper presents a Wind turbine (WT) system based on Permanent magnet synchronous generator (PMSG) using Surface mounted synchronous generator (SPMSG) and Interior magnet synchronous Generator (IPMSG). The analysis is compared between IPMSG and SPMSG. The same amount of copper and iron were used in both generators. In order to broaden the investigation two different appropriate motors have been used. This paper shows the analysis between both SPMSG and IPMSG technique. The copper and iron losses were utilized with machine and inverter loss in SPMSG and IPMSG technique. The SPMSG and IPMSG are compared based on density of power, electrical efficiencies, losses and torque. The angle of voltage, current and power were contributed in both IPMSG and SPMSG technique. In this technique the Back to back converter was utilized in the PMSG system it is utilized to change the power into dc-link. Simulation result shows the comparison of SPMSG and IPMSG technique with WT system and experimental results are obtained based on the power input at the shaft of the generator.

Index Terms: Back to Back converter, IPMSG, PMSG, SPMSG, Stator current, WT.

1 INTRODUCTION

Nwind turbine (WT) system the permanent magnet synchronous generators (PMSG) are mostly used because, compared to other generators it has high torque for weighting the ratio. In PMSG also has high efficiency, less maintenance cost and it has no slip rings. In PMSG has two types of magnets were noticed. The first magnet is mounted on the surface so it is named as SPMSG the second magnet is placed inside the rotor so it is named as IPMSG. Compared to SPMSG the IPMSG has higher torque and it has thick magnets. The vibration and production of noise in SPMSG is less than IPMSG. Four different kinds of SPMSG and IPMSG generators are produced to present PMSG in wind power generation system. It is essential to have less wind speed with high proficiency in WT applications. Investigation of different operating point in the system is necessary. The SPMSG and IPMSG are compared based on density of power, electrical efficiencies, losses and torque. Various magnets were used to increase same power in PMSG system. It is the interesting aspect in this method in the event that the SPMSG and IPSMG system increase same measure of magnets. In the WT system the fault ride through (FRT) is one of the important issues of operating system. The grid connection requirements (GCRs) involve the operational condition control of the distributed power system. The efficiency and reliability are provided from the GCRs to electrical grid system. Variable speed of WT generator is necessary to obtain maximum power from the fluctuating wind. A sophisticated control strategy requires for this generator. During grid faults, the WT must be connected to the electrical grid system. WT supplies electrical power grid system (2) During fault condition WT will inject a reactive power to recover the grid voltage (3) After the grid fault condition; WT starts the delivery of active power. During grid fault, these conditions are used to increase the stability of WT. To increase the capability of PMSG various methods are presented in FRT. Based on wind energy conversion system (WECS) a braking chopper (BC) system has implemented to improve the capacity of FRT in PMSG during grid fault. In this method some of the advantages were described like: Control structure is simple and cost is low, but BC system does not increase the quality of power in the output of WT system. WT system is developed based on PMSG for the generator side converter with output maximization. The switching mode generator is used for small scale WT system. The generator side switch mode rectifier is operated to gain more power from the wind. In this method an IGBT is required as an active switching device, which is used to control the generator torque to produce maximum power. A Static synchronous compensator (STATCOM) was introduced to evaluate the dynamic mechanism of the system in the WT system. Soft computing method was implemented in wind power applications such as: generation of wind power, power control of WT, MPPT. This method is not efficient in WT system. Remainder of the paper is depicted as follows: Section 2 Clarifies the recent research work. Section 3 clarifies the modelling of wind turbine permanent magnet synchronous generator. Section 4 depicts the overview of proposed system set up. Section 5 depicts the operations and functions of PMSG. Section 6 depicts the Simulation Result and discussion. Section 7 concludes the paper.

2 RECENT RESEARCH WORK: A BRIEF REVIEW

All Various research works have previously existed in the literature, based on the performance of permanent magnet wind turbine generator. Some of them were reviewed here. F.Z. Naama et al. [1] have presented a PMSG with WT system. This technique was used in WT to work automatically based on wind speed. Specifically PMSG was modeled in the WT system. Because of the improvement of WER the dynamic conduct of power system will change infinitely. U. Karaagac et l. a [2] have shown an Electromagnetic transient (EMT) system for full size converter and it was utilized to analyze the

- *Mr. Dhas Bensam Samraj, Research Scholar, Department of Electrical and Electronics Engineering, Govt. College of Technology, Coimbatore, India E-mail: dhasbensam0629@gmail.com*
- *Dr. Maruthu Pandi Perumal, Assistant professor, Department of Electrical and Electronics Engineering, Govt. College of Technology, Coimbatore, India*

dependability. For the recreation and transient conduct of wind park system, the WT based full time converter comprises of some nonlinearities and creation capacities. At PMSG the topology was utilized in the system. N.A. Bhuiyan and A. M. Donald [3] have displayed a PMSG which was a main target of the system. The cost of WT power was high in the system compared to Energy. The structure of SPMSG was planned and it was utilized to expand the power rates up to 10MW. It demonstrated from the system of magnet and produced lower measure of energy. A thermal model was introduced to calculate the temperature of air cooling and to reduce the temperature of magnet from120^0 to 80^0. When utilizing less expensive temperature it diminishes the loss of wind and increment the magnet as effective. In view of PMSG, A. Gencer [4] has introduced a fuzzy logic control (FLC) system to improve the dependability of the system during the deficiency of grid. The FLC system was intended to expand the presentation deficiency in the WT. In WT, the FLC system was executed to control both the machine side and grid side converters. In the method the FLC system was used under a few operational conditions. V. About the improvement method of a direct drive flux switching wind generator had portrayed by Dmitrievskii et al. [5]. In the procedure different objective functions were introduced, for example, power converter, loss of average and permanent magnet cost. During optimization a load profiles were displayed to decrease the efforts of the technique. During optimization, up to 30% the average loss was decreased and the normal deficiency was expanded up to 6%. The power of converter was reduced to 10%.B. Kim [6] had displayed a direct drive (DD) with PMSG for high power WT system. The greatest power system was acquired under WT. The PVSG system was displayed by utilizing correlation function and parameters. With limited component, the presentation qualities of the present generator were analyzed. S. Seralathan et al. [7] had introduced a horizontal axis small wind turbine (HAWT) with sharp blade tip control system utilizing PMSG.

2.1 Background of the Research Work

The PMSG in wind turbine system are the challenging task which is obtained from the recent research work. The PMSG technique was used here based on the wind speed. From PMSG it has introduced comparison between two generators that is SPMSG and IPMSG. Various approaches are presented to improve the dependability of the system during the deficiency of grid like fuzzy logic control (FLC), direct drive flux switching wind generator, horizontal axis small wind turbine (HAWT). The FLC is used in integrated and complex system; it has high precision and rapid operation. Lower speed and longer run time of the system and lack of real time response these all are the major drawback. The Direct drive wind generator is used to reduce the operating cost and also used to reduce the cost of maintenance. The Direct drive has large size drawback and it has heavy mass. Horizontal axis small wind turbine was used to gives the turbine blades at the optimum angle of attack and it gives high efficiency. But the drawback is it cannot move perpendicular to the wind. Several methodological works have not been exhibited in the literature to address this issue. These disadvantages and issues have motivated to do this research work.

3 Modelling of Wind Turbine Permanent Magnet Synchronous Generator

In wind turbine system the approaching wind generator is moved to mechanical generator in the PMSG procedure [8-10]. The back - back converter changes over the power into Dc link. At that point it will change over to the grid side converter. The PMSG procedure is for the most part utilized in the WT system. In PMSG technique the wind energy system is utilized to decrease the expense and weight and it is littler in size. The PMSG is directed by the generator in dynamic and receptive power [11-13]. Figure1. Block diagram of PMSG Wind turbine system. On the off chance that the grids convey the active power to the Dc-link, at that point it is utilized to keep up the voltage of Dc-link. The PMSG is relying upon the control of generator. Fig 1 demonstrates the block diagram of wind turbine system.

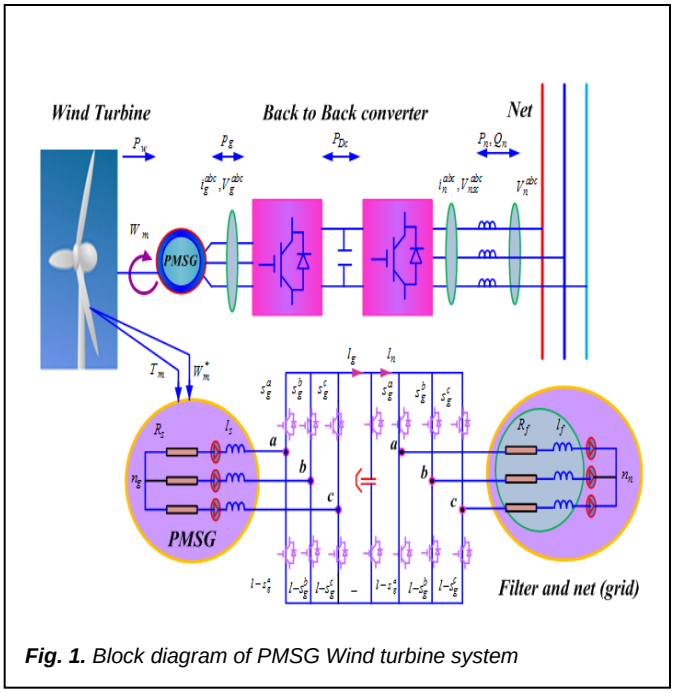

Fig. 1. *Block diagram of PMSG Wind turbine system*

3.1 Work Wind Turbine System

The Wind turbines (WT) are generally separated from the system to protect themselves from over current and voltage brought about by unbalanced grid conditions [14, 15]. Thus it cannot catch the total amount of wind energy [16, 17]. Subsequently, the system controller has to relieve the adverse impact on the WT [18, 19]. In the rotating of rotor, the wind changes the kinetic energy from moving into mechanical vitality which is shown as follows,

$$p_{WT} = \frac{1}{2} R_A \rho Cp(\delta,\phi) V_w^2 \quad (1)$$

where the effective area of blade is denoted as R_A, the density of air is denoted as ρ. The coefficient of power is represented as Cp, ϕ is the pitch angle, the speed of wind is denoted as V_w and it is represented in equation (2) as follows. The coefficient of Damp is denoted as d, is

$$\phi = \frac{\omega_R}{V_w}$$

(2)

At peak level, the wind powers get its optimum value of Cp at equation (1). In rotor speed, the maximum value of speed ratio is δ . The operating mode of WT is shown in Fig 2.

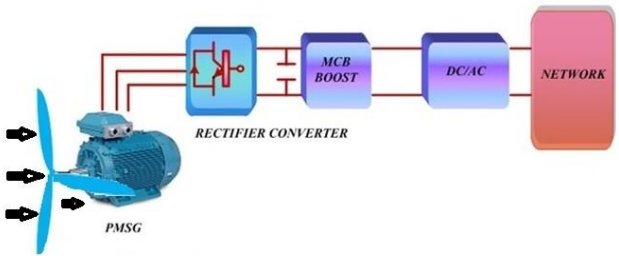

Fig. 1. *Operating mode of WT*

In wind turbine system the motion were produced from the permanent magnets which are curved in shape through the hole. The wind is displayed at before the turbine and the most extreme power is picked up from the wind sensor and it extricated from the WT.

3.2 Permanent-Magnet Synchronous Generator

The PMSG is generally utilized in WT system [20-23]. In this system the saliency and the response of armature isn't utilized. In a Permanent magnet generator, the magnetic field of the rotor is delivered by permanent magnets. Different kinds of generator use electromagnets to create an attractive field in a rotor winding. The immediate current in the rotor field winding is nourished through a slip-ring get together or gave by a brushless exciter on a similar shaft. Superior lasting magnets themselves have basic and warm issues. Torque current MMF vector ally joins with the persevering transition of permanent magnets, which prompts higher air-hole motion thickness and in the long run, center immersion. In these permanent magnet alternators the speed is straight forwardly relative to the yield voltage of the alternator. The mathematical modelling of PMSG appeared as pursues,

$$T_g^{dq}(s)=\begin{pmatrix} P_s & 0 \\ 0 & P_s \end{pmatrix} I_g^{dq}(s)+\frac{d\Psi^{dq}(s)}{ds}+\begin{pmatrix} 0 & -\omega_e(s) \\ \omega_e(s) & 0 \end{pmatrix}\Psi^{dq}(s) \quad (3)$$

where $T_g^{dq}(s)=(T_g^d(s),T_g^q(s))$ is the output voltage of the generator, P_s is denoted as the resistance of stator. $\Psi^{dq}(s)$ is represented as follows

$$\Psi^{dq}(s)=\begin{pmatrix} M_s & 0 \\ 0 & M_s \end{pmatrix} I_g^{dq}+\begin{pmatrix} \Psi_m \\ 0 \end{pmatrix}$$

(4)

$\Psi^{dq}(s)$ is denoted as the linkage of flux generator.

3.3 Back to back Converter

Back-back converter is one of the power molding devices. It is utilized to change over the machines. It was characterized dependent on the kind of converter based on its design. The back – back converter was commonly utilized in energy conversion methods [24]. The back – back converter is utilized in voltage, current and power sources. In back-back converter are indicated as the star point in the star association [25-27]. The output voltage of phase side and system side converter is described as pursues,

$$V_g^{abc}=\frac{\mathbf{V}dc}{3}S_g^{abc}M^{abc}, V_{nsc}^{abc}=\frac{\mathbf{V}dc}{3}S_n^{abc}M^{abc}$$

(5)

here S_g^{abc} and S_n^{abc} are denoted as the switching vector in both the phase side and grid side converter. M^{abc} is represented as the matrix function of transformation.

4. Overview of Proposed System Set Up

In this system it shows the speed of WT based PMSG. The Dc link is connected to converter else to the grid. Here the IGBT technique was utilized [1-5]. IGBT is used to gain the desirable current and voltage with series and parallel [6, 7, 28].

4.1. Design and loss of machine

The SPMSG cross section is shown in Fig 3. This paper shows the losses of machine, iron and copper. Loss of other machines was ignored [29-30]. The temperature of the machine during operating condition is 75^0C. The both machines of IPMSG and SPMSG have the same USAGE of material and dimensions [31-35].

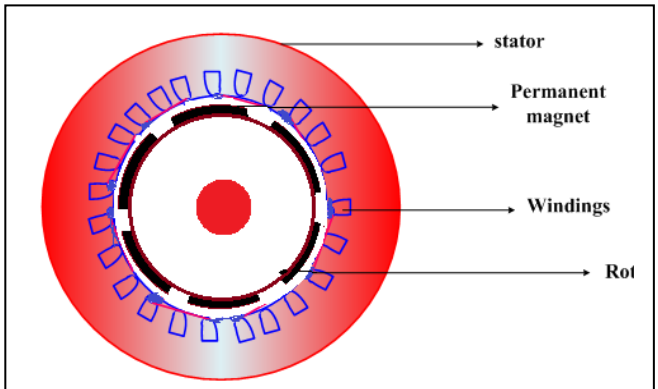

Fig. 3*. Cross section of SPMSG*

The placement of magnet is different in both machines. The calculation of losses in iron is depicted as below.

$$P_{fe}=KW_{El}^2$$

(6)

The loss of iron is represented as P_{fe} , constant K and the rate of speed in SPMSG is denoted as 0.0919 and in IPMSG is denoted as 0.0878. The speed of machine is represented as W_{El}^2 . The calculation of losses in copper is shown below, and the cross section of IPMSG is shown in Fig 4.

$$P_{Cu}=3r_5|I_S|^2$$

(7)

Here, P_{Cu} is denoted as the loss of copper, the phase resistance of the armature is represented as r_5 . The RMS value of magnitude is depicted as $|I_S|$.

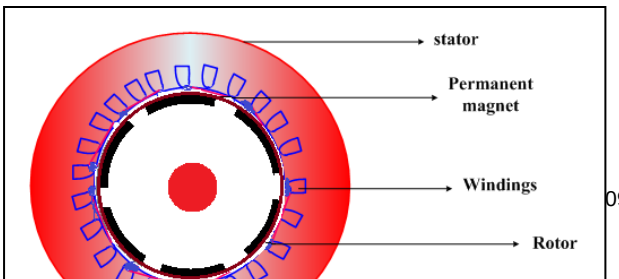

4.2. IGBT's with power electronic converter (PEC)

The 6pulse transisting converter is utilized in PEC in the module of IGBT. A high power WT system is exhibited in IGBT with various speed of wind for the efficiency and loss of the system [36]. In this system the current value of RMS is equivalent to the estimation of evaluated current. The two estimations of current is signified as pursues,

$$I_{rated}\ RMS = \frac{I_{ref}}{2}$$

(8)

From the above equation it is noted that through the water cooling converter the adequate heat is transferred [37]. In both IGBT and in diode, the conduction loss and switching loss are the dominant losses. The loss of converter is calculated as shown below

$$IGBT_{Cond} = \left(\frac{M\sin\varphi}{8} + \left(\frac{1}{2}\right)\right) V_{ceo}.I_1 + \left(\frac{M\sin\varphi}{3\pi} + \left(\frac{1}{8}\right)\right) R_{ce}.I_1^2$$

(9)

$$D_{cond} = \left(\frac{M\sin\varphi}{8} - \left(\frac{1}{2\pi}\right)\right) V_{fo}.I_1 + \left(\frac{M\sin\varphi}{3\pi} - \left(\frac{1}{8}\right)\right) R_f.I_1^2$$

(10)

$$IGBT_{Sw} = FE_{sw-}\left(\frac{I_1}{I_{ref}}.\frac{1}{\pi}\right)^{ki} \cdot \left(\frac{V_{cc}}{V_{ref}}\right)^{kv}$$

(11)

$$D_{Sw} = FE_{sw-}\left(\frac{I_1}{I_{ref}}.\frac{1}{\pi}\right)^{ki} \cdot \left(\frac{V_{cc}}{V_{ref}}\right)^{kv}$$

(12)

$$E_{sw} = IGBT\_On + IGBT\_Off$$

(13)

Here from equations $IGBT_{cond}$ and D_{cond} are denoted as the conduction loss in IGBT and diode. The scaling parameters are represented as k_i and k_v. R_{ce} and R_f are denoted as the resistive values of semiconductor. $IGBT_{Sw}$ and D_{Sw} are denoted as the switching loss of IGBT and diode. The power factor is denoted as $Sin\varphi$. Then I_1 is denoted as the peak value of stator current and which is calculated as follows

$$I_1 = \frac{|I_s|}{N_{parallel}}$$

(14)

Where, $|I_s|$ is denoted as the stator current of magnitude and $N_{parallel}$ is derived as follows

$$n_{parallel} = \frac{M(|I_s, RMS|)}{I_{rated}, RMS}$$

(15)

Where, $M(|I_s, RMS|)$ is represented as the magnitude of maximum stator current. I_{rated}, RMS is equated from equation (7). E_{sw}_IGBT and E_{sw}_D are represented as the switching loss of transistor and diode. The determination of dc-link voltage is described as below

$$V_{Dc} = \frac{2V_{ac}}{0.95}$$

(16)

From the above equation V_{ac} represents the voltage of machine as neutral. From equation (15) the voltage of dc-link becomes constant. The series number of modules is characterized as follows, from the equations both the series and parallel modules of SPMSG and IPMSG are utilized to achieve the dc-link voltage.

$$N_{series} = \frac{V_{Dc}}{V_{ref}}$$

(17)

5 Operations and Functions of PMSG

There is no saliency was available in the IPMSG system. In this kind of machine the subsequent term ends up zero [38]. By the utilization of dynamic rectifier we can ready to control the voltage of machine. Depending upon the voltage, the converter and machines are working. At the point when the speed of wind is diminished then the speed of rotor likewise turns out to be low. In lower wind speed the lower voltage is used. Contrasted with SPMSG the IPMSG has low measure of copper losses. In IPMSG the loss of conduction and switching is low [38, 39]. The conditions for the PMSG-machine in dp-part structure can be made as pursues

$$U_{SD} = L_q i_{sq}\, w_{el} - R_s i_{sd}$$

(18)

$$U_{SQ} = L_d i_{sd}\, w_{el} + R_s i_{sq} + w_{el}\Psi m$$

(19

The equation of torque is given as follows

$$T_e = \frac{3}{2} p\left[\Psi_m i_{sq} + i_{sq} i_{sd}\left(L_d - L_q\right)\right]$$

(20)

5.1. Power Factor (PF) calculation

In PF the angle of voltage is calculated and denoted as follows;

$$\varphi u = Cos^{-1}\left(\frac{U_{sd}}{U_{sq}}\right)$$

(21)

The U_{sd} and U_{sq} are taken from equation (17) and (18). The angle of current is represented as φu. From here the angle of power factor is the difference between both the angle current and voltage.

6 Result and Discussion

In the following chapter, the simulation finding of the suggested method is evaluated. The performance of SPMSG and IPMSG by the suggested PMSG method is analyzed and implemented. To check the efficiency of the suggested method, the output of the SPMSG and IPMSG is evaluated. In SPMSG and IPMSG both the copper and iron loss was described. The SPMSG and IPMSG was portrayed the Maximum and Inverter losses with wind speed and also the

comparison of voltage, current and power angle with SPMSG and IPMSG was also analyzed . During different working modes and occurrences, the system is screened to check its efficiency. In the following chapter, the simulation finding of the suggested method is evaluated. Fig 5 shows the experimental set up of SPMSG and IPMSG. A prime mover and load adjusting device is provided to adjust the turbine equivalent power input at the shaft of the generator for various wind speeds. Torque and proximity sensor are mounted in the setup. Circuit breakers, prime mover speed control and multifunction meters are provided in the panel. In SPMSG and IPMSG technique the copper and iron losses were utilized with machine and inverter loss. Compared to SPMSG the IPMSG has higher torque and it has thick magnets. The SPMSG and IPMSG are compared based on density of power, electrical efficiencies, losses and torque. Various magnets were utilized to increase same power in PMSG system.

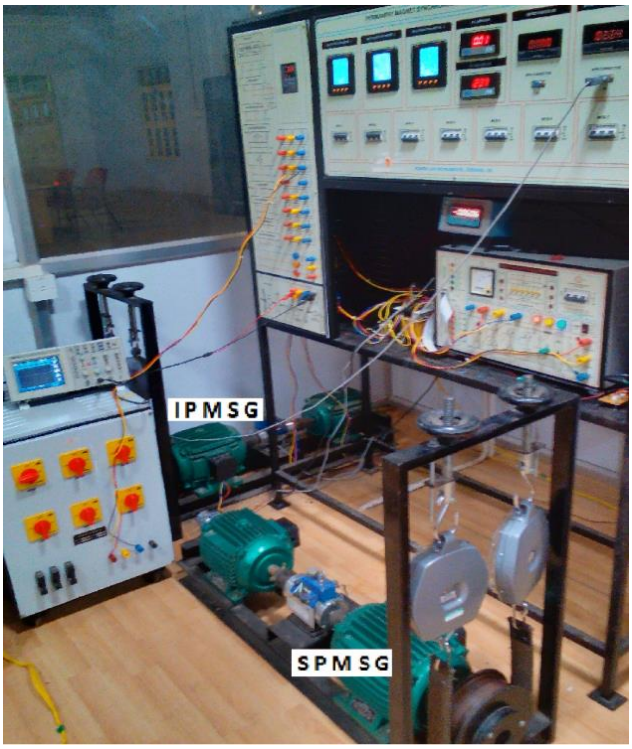

***Fig. 5**. Hardware of SPMSG and IPMSG*

The analysis of machine loss for SPMSG and IPMSG techniques were shown in Fig 6. In this graph the machine loss of SPMSG and IPMSG Copper and iron losses were portrayed. At the wind speed of 5 to 7(m/s) the copper loss of SPMSG is increased up to 2 - 6.9W and it remain constant till the end. The iron loss of SPMSG is portrayed from the wind speed of 5m/s from 0-1.9w and it remains constant till the end. In Fig 4 the copper loss of IPMSG is increased at the wind speed of 5 to 9m/s from 0 to 4.2w and it remains constant. The iron loss of IPMSG is analysed at the wind speed of 5-6m/s from 1 to 1.5w and it remains constant till the end of the operation. In Fig 7 the Analysis of Inverter loss for SPMSG and IPMSG techniques is portrayed. From this graph the copper and iron loss of SPMSG and IPMSG was analyzed. The copper loss of SPMSG in inverter loss from 0 to 4.5w and suddenly it reduced up to 4.5 to 2.9 at the wind speed of 5 to 10m/s, and it remains constant till the end of operation. The iron loss of SPMSG is analyzed. The loss of iron in SPMSG is from 0 to 2.5w at the wind speed 5-10m/s and it remains constant.

***Fig. 6.** Analysis of Machine loss for SPMSG and IPMSG*

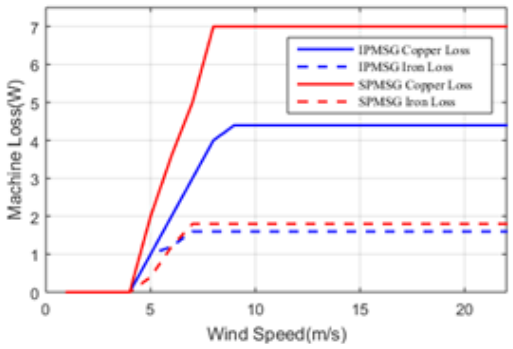

***Fig. 7.** Analysis of Inverter loss for SPMSG and IPMSG*

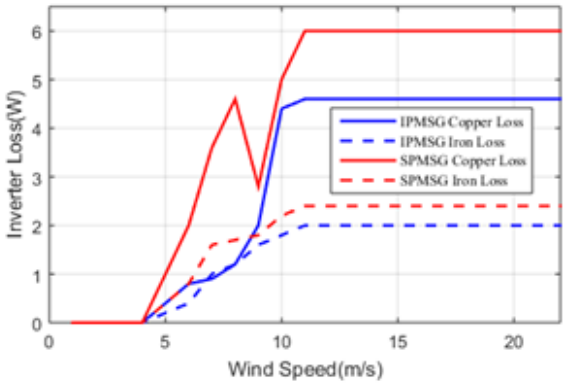

The copper loss of IPMSG is portrayed from 0 to 4.3w at the wind speed of 5 to 10m/s, and then it remains constant. The iron loss of IPMSG at the speed of 5-10 m/s from 0 to 2w, and then it remains constant till the end of the operation. The machine and inverter loss is analyzed under SPMSG and IPMSG copper and iron losses and also the votage, current and power factor angle of SPMSG and IPMSG are also described. The machine loss of SPMSG and IPMSG copper and iron loss was illustrated in Fig 8. The copper loss of SPMSG is analyzed from 0 to 8.5w at the wind speed of 5 to 10.5m/s and it remains constant till the end. The iron loss of SPMSG is illustrated from 1w at the speed of 5 to 9m/s and then it remains constant. The copper Loss IPMSG is illustrated from 2 to 6.5w at the wind speed of 5 to 10.2m/s and then it remains constant. The iron loss of IPMSG is assigned from 1w at the wind speed 5 to 10m/s and then it remains constant till the end of the operation.

Fig. 8. *Analysis of Machine loss for SPMSG and IPMSG*

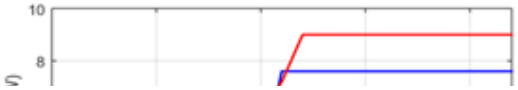

Fig. 9. *Analysis of Inverter loss for SPMSG and IPMSG*

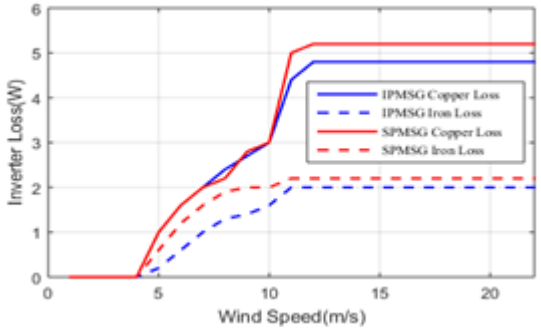

Fig. 10. *Comparison of Voltage, current and power factor angle of SPMSG*

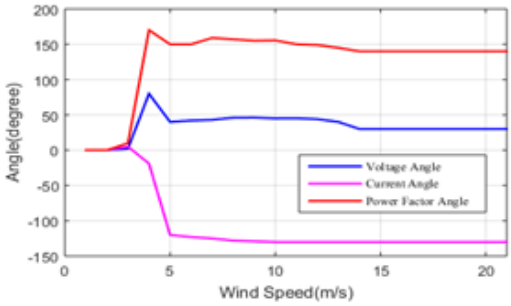

In Fig 9 the analysis of inverter loss with SPMSG and IPMSG for copper and iron loss is portrayed. In inverter loss the copper loss of SPMSG was analyzed from 0 to 5w at the wind speed of 5 to 10.5m/s and then it remains constant. The iron loss of SPMSG is portrayed at the wind speed of 5 to 10m/s from 0 to 2w and it remains constant till the end of operation. The copper loss of IPMSG in inverter loss is portrayed as at the wind speed of 5 to 10.5m/s from 0 to 4.5w and it remains constant till the end of the operation. The iron loss of IPMSG is potrayed from 0 to 1.9w at the wind speed of 5 to 10.1m/s and it remains constant.In Fig 10 the comparison of voltage, current and power angle of SPMSG is analyzed. In this graph the votage, current and power angle is illustrated with a speed of wind. In voltage the angle is optimized from 0 to 50.5degree and suddenly it reduced at the wind speed of 5 to 10.9m/s and then it remains constant till the end. In current the degree of angle is decreased up to -100degree and then it remains constant. In power the degree of angle is increased up to 150.5degree at the wind speed of 5 to 10.5m/s and then it remains constant.

Fig. 11. *Comparison of Voltage, current and power factor angle of IPMSG*

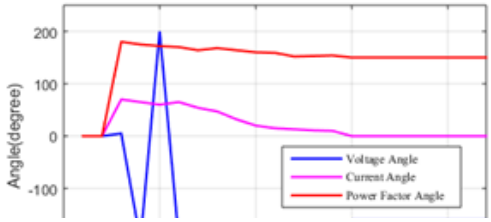

Fig.12 *Comparison of Torque in SPMSG and IPMSG*

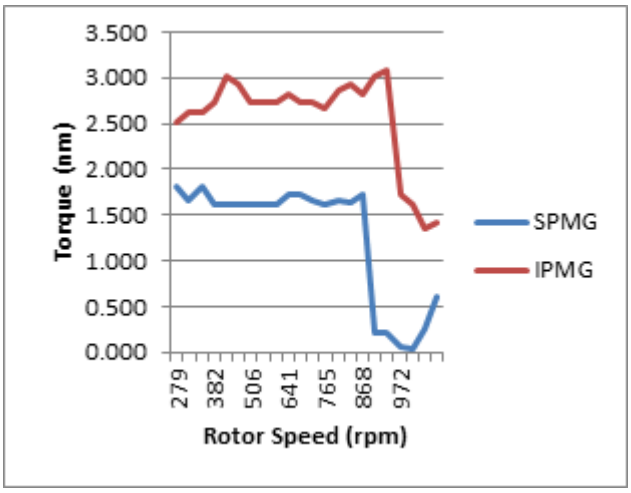

In Fig 11 the comparison of voltage, current and power angle of IPMSG is analyzed. In this graph the votage, current and power angle is illustrated with a speed of wind. In voltage the angle is decreased up to -200 degree and suddenly it optimized from up to 200degree and suddenly it reduced at the wind speed of 5 to 10.9m/s and then it remains constant till the end. The maximum current of IPMSG is 0 to 15degree and then it remains constant. In power the degree of angle is increased up to 100.5degree at the wind speed of 1 to 15m/s and then it remains constant. Fig 12 to Fig 17 shows the experimental analysis of rotor speed with torque, frequency, line voltage, line current, power factor, active and reactive power in SPMSG and IPMSG.

Fig. 13*. Comparison of Frequency in SPMSG and IPMSG*

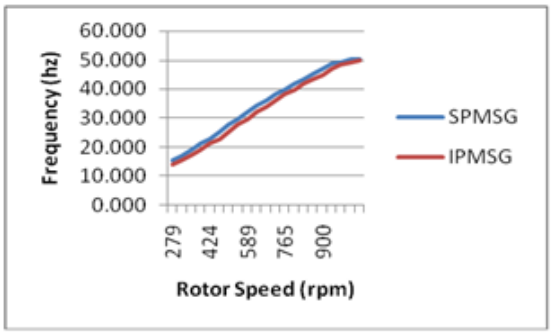

Fig. 14 *comparison of Line voltage in SPMSG and IPMSG*

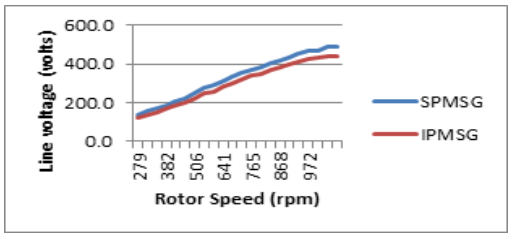

Fig. 15. *Comparison of Line current in SPMSG and IPMSG*

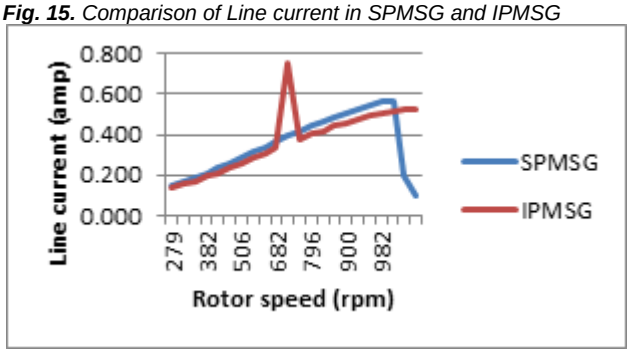

Fig. 16. *comparison of Power factor in SPMSG and IPMSG*

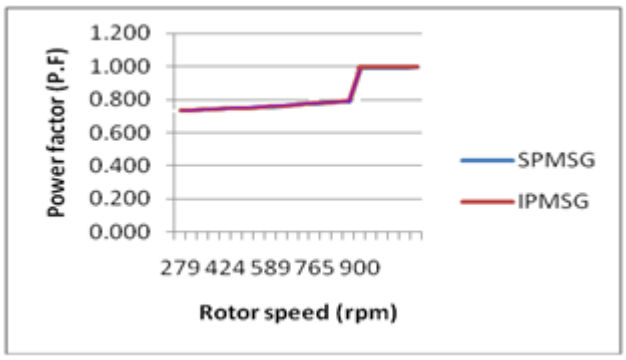

Fig. 17. *Comparison of Active and Reactive power in SPMSG and IPMSG*

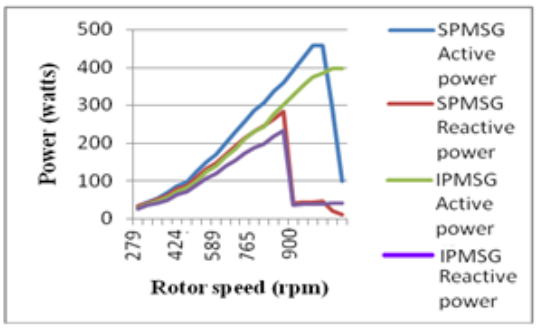

TABLE 1

SURFACE MOUNTED PERMANENT MAGNET SYNCHRONOUS GENERATOR

Surface Mounted Permanent magnet synchronous generator

Torque(nm)	Rotor Speed (rpm)	Frequency (Hz)	Line voltage (Volts)	Line current (Ampere)	Power Factor	Active power (watts)	Reactive power (watts)
1.515	279.312	13.966	136.2	0.149	0.734	34	32
1.664	310.347	15.517	154.6	0.171	0.736	45	41
1.515	341.381	17.069	170.8	0.191	0.738	55	51
1.614	382.761	19.138	187.7	0.212	0.741	68	61

TABLE 2

INTERIOR PERMANENT MAGNET SYNCHRONOUS GENERATOR

Interior Permanent magnet synchronous generator

Torque (nm)	Rotor Speed (rpm)	Frequency (Hz)	Line voltage (Volts)	Line current (Ampere)	Power Factor	Active power (watts)	Reactive power (watts)
2.521	279.312	13.966	123.3	0.135	0.733	27	25
2.622	310.347	15.517	139.6	0.155	0.735	36	34
2.622	341.381	17.069	150.7	0.170	0.737	44	40
2.723	382.761	19.138	169.5	0.193	0.739	54	49
3.025	424.140	21.207	184.0	0.211	0.743	71	64
2.925	455.175	22.759	202.2	0.233	0.743	80	71
2.723	506.899	25.345	222.5	0.260	0.749	99	88
2.723	558.624	27.931	247.5	0.291	0.754	123	107
2.723	589.659	29.483	259.3	0.305	0.757	139	120
2.824	641.383	32.069	283.5	0.335	0.762	165	140
2.723	682.763	34.138	301.4	0.356	0.766	184	155
2.723	724.142	36.207	319.3	0.380	0.771	209	173
2.672	765.522	38.276	338.9	0.404	0.776	231	188
2.874	796.556	39.828	349.7	0.418	0.779	244	197
2.925	837.936	41.897	369.6	0.443	0.785	276	218
2.824	868.970	43.449	382.0	0.458	0.790	301	233
3.025	900.005	45.000	395.6	0.475	0.995	328	35
3.076	941.385	47.069	411.1	0.494	0.995	353	38
1.714	972.419	48.621	423.5	0.508	0.995	374	38
1.614	982.764	49.138	432.4	0.518	0.995	385	38
1.361	1000.351	50.018	436.7	0.522	0.995	397	39
1.412	1003.454	50.173	437.8	0.524	0.995	398	39

Table 1 represents the SPMSG with the functions of torque, rotor speed, frequency, line voltage, line current, power factor, active and reactive power. Table 2 represents the IPMSG with the functions of torque, rotor speed, frequency, line voltage, line current, power factor, active and reactive power. The analyzed result shows that compared to SPMSG the IPMSG performs better.

4 CONCLUSION

The SPMSG and IPMSG technique with WT system is considered in this work. The Size of SPMSG and IPMSG are same. This paper examines the modelling of IPMSG and SPMSG techniques. Simulation result shows the comparison of SPMSG and IPMSG technique with WT system. The both machines are connected with the IGBT converter. The Machine loss and inverter losses were described with different wind speed. The execution is compared with the copper and iron losses. From the simulation result the average energy of machine is higher for IPMSG compared to SPMSG using dc-link voltage. The efficacy of the suggested approach is evaluated through the use of comparison assessment with alternative approaches such as IPMSG copper and iron losses, SPMSG copper and iron losses. The result of the

comparison indicates that over the other existing systems the suggested strategy is extremely skilled. Finally in both simulation and experimental analysis demonstrates the outcome of IPMSG WT system is high compared to SPMSG WT system.

ACKNOWLEDGMENT

The authors thank National Project Implementation Unit established by Ministry of Human Resource Development, Government of India for supporting this project by providing experimental facilities for conducting this research related issues under Technical Education Quality Improvement Programme II.

REFERENCES

[1] F. Naama, A. Zegaoui, Y. Benyessad, F. Kessaissia, A. Djahbar, and M. Aillerie, "Model and Simulation of a Wind Turbine and its Associated Permanent Magnet Synchronous Generator," Energy Procedia, vol. 157, pp. 737-745, 2019.

[2] U. Karaagac et al., "A Generic EMT-Type Model for Wind Parks with Permanent Magnet Synchronous Generator Full Size Converter Wind Turbines," IEEE Power and Energy Technology Systems Journal, vol. 6, no. 3, pp. 131-141, 2019.

[3] N. Bhuiyan, and A. McDonald, "Optimization of Offshore Direct Drive Wind Turbine Generators with Consideration of Permanent Magnet Grade and Temperature," IEEE Transactions on Energy Conversion, vol. 34, no. 2, pp. 1105-1114, 2019.

[4] A. Gencer, "Analysis and Control of Fault Ride-Through Capability Improvement for Wind Turbine Based on a Permanent Magnet Synchronous Generator Using an Interval Type-2 Fuzzy Logic System," Energies, vol. 12, no. 12, p. 2289, 2019.

[5] V. Dmitrievskii, V. Prakht, and V. Kazakbaev, "Design Optimization of a Permanent-Magnet Flux-Switching Generator for Direct-Drive Wind Turbines," Energies, vol. 12, no. 19, p. 3636, 2019.

[6] Kim, "Design Method of a Direct-Drive Permanent Magnet Vernier Generator for a Wind Turbine System," IEEE Transactions on Industry Applications, vol. 55, no. 5, pp. 4665-4675, 2019.

[7] S. Sivamani et al., "Experimental data on analysis of a horizontal axis small wind turbine with blade tip power system using permanent magnetic generator," Data in Brief, vol. 23, p. 103716, 2019.

[8] K. Sze, and X. Liu, "Fabric drape simulation by solid-shell finite element method," Finite Elements in Analysis and Design, vol. 43, no. 11-12, pp. 819-838, 2007.

[9] S. Bai, and Z. Chang, "Analysis and Design of Low-Speed Direct-Driven Permanent-Magnet Submersible Motor," DEStech Transactions on Computer Science and Engineering, 2017.

[10] A. EL-Refaie, "Fractional-Slot Concentrated-Windings Synchronous Permanent Magnet Machines: Opportunities and Challenges," IEEE Transactions on Industrial Electronics, vol. 57, no. 1, pp. 107-121, 2010.

[11] R. Billinton, Y. Gao, and R. Karki, "Composite System Adequacy Assessment Incorporating Large-Scale Wind Energy Conversion Systems Considering Wind Speed Correlation," IEEE Transactions on Power Systems, vol. 24, no. 3, pp. 1375-1382, 2009.

[12] P. Reddy, A. El-Refaie, K. Huh, J. Tangudu, and T. Jahns, "Comparison of Interior and Surface PM Machines Equipped With Fractional-Slot Concentrated Windings for Hybrid Traction Applications," IEEE Transactions on Energy Conversion, vol. 27, no. 3, pp. 593-602, 2012.

[13] Y. Li, Z. Xu, and K. Wong, "Advanced Control Strategies of PMSG-Based Wind Turbines for System Inertia Support," IEEE Transactions on Power Systems, vol. 32, no. 4, pp. 3027-3037, 2017.

[14] Z. Zhang, F. Wang, J. Wang, J. Rodriguez, and R. Kennel, "Nonlinear Direct Control for Three-Level NPC Back-to-Back Converter PMSG Wind Turbine Systems: Experimental Assessment With FPGA," IEEE Transactions on Industrial Informatics, vol. 13, no. 3, pp. 1172-1183, 2017.

[15] M. Abdelrahem, C. Hackl, and R. Kennel, "Simplified model predictive current control without mechanical sensors for variable-speed wind energy conversion systems," Electrical Engineering, vol. 99, no. 1, pp. 367-377, 2016.

[16] A. Gencer, "Analysis and Control of Low-Voltage Ride-Through Capability Improvement for PMSG Based on an NPC Converter Using an Interval Type-2 Fuzzy Logic System," Elektronika ir Elektrotechnika, vol. 25, no. 3, pp. 63-70, 2019.

[17] S. Alepuz, A. Calle, S. Busquets-Monge, S. Kouro, and B. Wu, "Use of Stored Energy in PMSG Rotor Inertia for Low-Voltage Ride-Through in Back-to-Back NPC Converter-Based Wind Power Systems," IEEE Transactions on Industrial Electronics, vol. 60, no. 5, pp. 1787-1796, 2013.

[18] M. Hossain, "A non-linear controller based new bridge type fault current limiter for transient stability enhancement of DFIG based Wind Farm," Electric Power Systems Research, vol. 152, pp. 466-484, 2017.

[19] A. Beltran-Pulido, J. Cortes-Romero, and H. Coral-Enriquez, "Robust Active Disturbance Rejection Control for LVRT capability enhancement of DFIG-based wind turbines," Control Engineering Practice, vol. 77, pp. 174-189, 2018.

[20] Rini Ann Jerin, P. Kaliannan, and U. Subramaniam, "Improved fault ride through capability of DFIG based wind turbines using synchronous reference frame control based dynamic voltage restorer," ISA Transactions, vol. 70, pp. 465-474, 2017.

[21] Gencer, "Analysis and Control of Fault Ride through Capability Improvement PMSG Based on WECS Using Active Crowbar System during Different Fault Conditions," Elektronika ir Elektrotechnika, vol. 24, no. 2, 2018.

[22] J. Conroy, and R. Watson, "Low-voltage ride-through of a full converter wind turbine with permanent magnet generator," IET Renewable Power Generation, vol. 1, no. 3, p. 182, 2007.

[23] S. Yang, T. Zhou, D. Sun, Z. Xie, and X. Zhang, "A SCR crowbar commutated with power converter for DFIG-based wind turbines," International Journal of Electrical Power & Energy Systems, vol. 81, pp. 87-103, 2016.

[24] M. Nasiri, J. Milimonfared, and S. Fathi, "A review of low-voltage ride-through enhancement methods for permanent magnet synchronous generator based wind turbines," Renewable and Sustainable Energy Reviews, vol. 47, pp. 399-415, 2015.
[25] H. Geng, L. Liu, and R. Li, "Synchronization and Reactive Current Support of PMSG-Based Wind Farm During Severe Grid Fault," IEEE Transactions on Sustainable Energy, vol. 9, no. 4, pp. 1596-1604, 2018.
[26] M. Nasiri, and R. Mohammadi, "Peak Current Limitation for Grid Side Inverter by Limited Active Power in PMSG-Based Wind Turbines During Different Grid Faults," IEEE Transactions on Sustainable Energy, vol. 8, no. 1, pp. 3-12, 2017.
[27] D. Yehia, D. Mansour, and W. Yuan, "Fault Ride-Through Enhancement of PMSG Wind Turbines With DC Microgrids Using Resistive-Type SFCL," IEEE Transactions on Applied Superconductivity, vol. 28, no. 4, pp. 1-5, 2018.
[28] O. Alizadeh, and A. Yazdani, "A Strategy for Real Power Control in a Direct-Drive PMSG-Based Wind Energy Conversion System," IEEE Transactions on Power Delivery, vol. 28, no. 3, pp. 1297-1305, 2013.
[29] H. Polinder, F. Van Der Pijl, G. De Vilder, and P. Tavner, "Comparison of Direct-Drive and Geared Generator Concepts for Wind Turbines," IEEE Transactions on Energy Conversion, vol. 21, no. 3, pp. 725-733, 2006.
[30] S. Li, T. Haskew, R. Swatloski, and W. Gathings, "Optimal and Direct-Current Vector Control of Direct-Driven PMSG Wind Turbines," IEEE Transactions on Power Electronics, vol. 27, no. 5, pp. 2325-2337, 2012.
[31] A. Ayad, P. Karamanakos, and R. Kennel, "Direct Model Predictive Current Control Strategy of Quasi-Z-Source Inverters," IEEE Transactions on Power Electronics, vol. 32, no. 7, pp. 5786-5801, 2017.
[32] A. Grimble, and A. Ordys, "Predictive control for industrial applications," Annual Reviews in Control, vol. 25, pp. 13-24, 2001.
[33] P. Cortes, M. Kazmierkowski, R. Kennel, D. Quevedo, and J. Rodriguez, "Predictive Control in Power Electronics and Drives," IEEE Transactions on Industrial Electronics, vol. 55, no. 12, pp. 4312-4324, 2008.
[34] F. Morel, Xuefang Lin-Shi, J. Retif, B. Allard, and C. Buttay, "A Comparative Study of Predictive Current Control Schemes for a Permanent-Magnet Synchronous Machine Drive," IEEE Transactions on Industrial Electronics, vol. 56, no. 7, pp. 2715-2728, 2009.
[35] P. Correa, M. Pacas, and J. Rodriguez, "Predictive Torque Control for Inverter-Fed Induction Machines," IEEE Transactions on Industrial Electronics, vol. 54, no. 2, pp. 1073-1079, 2007.
[36] Z. Cai, and Z. Guo, "Simulation and Analysis for New Contact System of Control and Protective Switching Based on Ansoft Maxwell," Applied Mechanics and Materials, vol. 229-231, pp. 1963-1966, 2012.
[37] S. Gunturi, and D. Schneider, "On the Operation of a Press Pack IGBT Module Under Short Circuit Conditions," IEEE Transactions on Advanced Packaging, vol. 29, no. 3, pp. 433-440, 2006.
[38] P. Roshanfekr, T. Thiringer, S. Lundmark, and M. Alatalo, "DC-link voltage selection for a multi-MW wind turbine," COMPEL - The international journal for computation and mathematics in electrical and electronic engineering, vol. 33, no. 5, pp. 1722-1740, 2014.
[39] A. McDonald, M. Mueller, and H. Polinder, "Structural mass in direct-drive permanent magnet electrical generators," IET Renewable Power Generation, vol. 2, no. 1, pp. 3-15, 2008.